



RESEARCH LETTER

10.1002/2017GL072996

Key Points:

- Coupling of Europa's ocean circulation and the ice shell impacts global stratification
- A low-latitude freshwater layer may suppress vertical heat and tracer transport
- Parameter space is explored based on properties observed by future missions

Supporting Information:

- Supporting Information S1

Correspondence to:

P. Zhu,
zhpeiyun@umich.edu

Citation:

Zhu, P., G. Manucharyan, A. F. Thompson, J. Goodman, and S. D. Vance (2017), The influence of meridional ice transport on Europa's ocean stratification and heat content, *Geophys. Res. Lett.*, 44, 5969–5977, doi:10.1002/2017GL072996.

Received 8 FEB 2017

Accepted 5 JUN 2017

Accepted article online 12 JUN 2017

Published online 22 JUN 2017

The influence of meridional ice transport on Europa's ocean stratification and heat content

Peiyun Zhu¹ , Georgy E. Manucharyan² , Andrew F. Thompson² , Jason C. Goodman³, and Steven D. Vance⁴ 

¹Department of Earth and Environmental Sciences, University of Michigan, Ann Arbor, Michigan, USA, ²Department of Environmental Science and Engineering, California Institute of Technology, Pasadena, California, USA, ³Department of Physics, Wheaton College, Norton, Massachusetts, USA, ⁴Jet Propulsion Laboratory, California Institute of Technology, Pasadena, California, USA

Abstract Jupiter's moon Europa likely hosts a saltwater ocean beneath its icy surface. Geothermal heating and rotating convection in the ocean may drive a global overturning circulation that redistributes heat vertically and meridionally, preferentially warming the ice shell at the equator. Here we assess the previously unconstrained influence of ocean-ice coupling on Europa's ocean stratification and heat transport. We demonstrate that a relatively fresh layer can form at the ice-ocean interface due to a meridional ice transport forced by the differential ice shell heating between the equator and the poles. We provide analytical and numerical solutions for the layer's characteristics, highlighting their sensitivity to critical ocean parameters. For a weakly turbulent and highly saline ocean, a strong buoyancy gradient at the base of the freshwater layer can suppress vertical tracer exchange with the deeper ocean. As a result, the freshwater layer permits relatively warm deep ocean temperatures.

1. Introduction

Jupiter's moon Europa is one of multiple confirmed ocean worlds [Nimmo and Pappalardo, 2016]. Evidence for an extant subsurface ocean comes from measurements by the *Galileo* spacecraft indicating an induced response to the changing direction of Jupiter's magnetic field, consistent with the existence of an electrical conductor near the surface [Kivelson *et al.*, 2000]. Based on gravity measurements, the rocky seafloor is 80–170 km below the surface [Anderson *et al.*, 1998]. The ocean is in communication with the surface on timescales shorter than 100 Myr, as indicated by Europa's complex surface geology [e.g., Pappalardo *et al.*, 1998] and sparsity of craters [Zahnle *et al.*, 2008]. This interaction controls the flux of surface-derived oxidants into the ocean [Vance *et al.*, 2016] and influences the ocean's dynamics in ways that have not been thoroughly evaluated to date. The ocean's composition, stratification, and circulation influence chemical exchange, such that an understanding of Europa's dynamical properties could help to assess whether Europa can support life [e.g., Schulze-Makuch and Irwin, 2002; Irwin and Schulze-Makuch, 2003].

Geothermal heat from the seafloor and loss of heat through the ice shell are critical mechanisms driving Europa's ocean circulation. Buoyant plumes confined by Coriolis forces may act to regionally transmit heat and materials directly between the seafloor and ice [Thomson and Delaney, 2001; Goodman *et al.*, 2004; Vance and Goodman, 2009]. However, larger-scale circulation features may develop through turbulent convection and through rotational constraints [Travis *et al.*, 2012; Soderlund *et al.*, 2014]. Critically, these prior studies have focused exclusively on the ocean and prescribed either a uniform surface temperature or a spatial distribution of surface heat fluxes.

The pole-to-equator temperature variation on Europa (~40 K) [Spencer *et al.*, 1999; Rathbun *et al.*, 2010] could support meridional variations in ice thickness that will also depend on the heat flux at the ocean-ice interface. The meridional ice thickness variations are estimated to be at most 3 km and zonal variations due to long-wavelength topography less than 7 km [Nimmo *et al.*, 2007]. Any variations in ice thickness will establish a pressure gradient, which can induce ice transport [Vance and Goodman, 2009]. This can occur by two mechanisms: the so-called ice pump [Lewis and Perkin, 1986] and down-thickness gradient ice flow [Goodman and Pierrehumbert, 2003].

Over sufficiently long timescales, thicker ice at the poles implies continuous transport of ice equatorward. At the equator (poles), the addition (removal) of ice requires preferential melting (growth) to maintain steady state conditions. In a weakly turbulent and saline ocean, freshwater fluxes at the equator can dilute the upper ocean to form a stable layer with lower salinity than the deep ocean, hence defined as a “freshwater” layer. In a dilute ocean [e.g., *Zolotov and Shock, 2001; McKinnon and Zolensky, 2003*] with buoyancy depending mainly on temperature, a freshwater lens can also be stable due to the negative thermal expansion coefficient of water for hydrostatic pressures less than ~ 25 MPa (Europa ice thickness less than ~ 17 km) [*Melosh et al., 2004*].

The strength and turbulent properties of Europa’s ocean circulation are uncertain. For example, *Soderlund et al. [2014]* demonstrates the possibility for an energetic convectively driven overturning ocean circulation that enhances the equatorial ocean heat fluxes. Other studies suggest alternative, less vigorous circulation regimes [e.g., *Vance and Goodman, 2009; Jansen, 2016*] with lower turbulent levels. However, these studies do not account for freshwater fluxes associated with the freezing/melting of the ice. Thus, the existence of the salt stratification of Europa’s ocean remains an open question.

Here we introduce a conceptual, two-column model to quantify the physical processes that may give rise to a freshwater layer beneath Europa’s ice shell. Using this model, we explore the sensitivity of the layer to key ocean characteristics, including its average salinity, the strength of the upper ocean turbulence, and the equator-to-pole ocean heat flux. The presence of a freshwater layer under the ice can suppress the efficiency of heat exchange with the deep ocean due to a buoyancy contrast at the interface between the layer and the deep ocean. We explore under which conditions this layer can influence deep ocean temperatures.

2. Model Description

Our approach is to develop a minimal model that captures the essential dynamics leading to the formation of compositional stratification in low-latitude regions of Europa’s ocean. An extreme but still insightful truncation is to consider two vertical columns, one at the equator (low latitudes) and one at the pole (high latitudes), to represent meridional gradients in ice thickness and ocean properties (Figure 1). An advantage of this approach is the derivation of analytical scalings that indicate the sensitivity (e.g., power law dependence) of the freshwater layer characteristics to Europa’s properties.

2.1. Ice Thickness Balance

The global heat budget governs the distribution of ice shell thickness. In our model, the positive heat flux from the ocean into the ice is transferred vertically through the ice by thermal diffusion. The temperature at the ocean-ice interface is fixed at the freezing point T_f , which may vary with pressure and salinity.

The ocean-ice heat flux F_{ocn} at the equator and the poles may be different, reflected in a parameter $\Delta F_{\text{ocn}} = F_{\text{ocn}}^e - F_{\text{ocn}}^p$; throughout this paper superscripts e and p denote variables of the equator and the pole columns, respectively. In studies by, e.g., *Goodman et al. [2004]* and *Jansen [2016]*, the ice is considered to be in a steady state governed by a one-dimensional vertical balance. However, positive lateral gradients in ice thickness will induce an equatorward ice or freshwater transport F_h (m s^{-1}) that results in ice formation at high latitudes and freshwater accumulation at low latitudes. Two physical mechanisms give rise to F_h : (i) down-gradient thickness transport [*Goodman and Pierrehumbert, 2003*] and (ii) the ice pump, which arises from the dependence of T_f on pressure (ice thickness) and composition [*Lewis and Perkin, 1986*]. By introducing F_h , we couple the ice dynamics to the ocean and are able to quantitatively explore their interactions.

The ice thickness balance is governed by

$$L \frac{dh^e}{dt} = \frac{\kappa_{\text{ice}}(T_f - T_s^e)}{h_0^e} + LF_h - (F_{\text{ocn}} + \Delta F_{\text{ocn}}), \quad (1)$$

$$L \frac{dh^p}{dt} = \frac{\kappa_{\text{ice}}(T_f - T_s^p)}{h_0^e + \Delta h} - LF_h - F_{\text{ocn}}, \quad (2)$$

where h^e and T_s^e (h^p and T_s^p) are the instantaneous ice thickness and surface temperature at low (high) latitudes, κ_{ice} is the thermal conductivity of ice, L is the latent heat of ice fusion (Table 1), h_0^e is the equilibrium ice thickness at the equator, and $\Delta h = h^p - h^e > 0$ is the pole-to-equator difference in the ice thickness. From left to right, the terms on the right-hand side of equations (1) and (2) represent the heat loss due to diffusion through the ice, the thickness flux caused by ice transport, and the ocean-ice heat flux.

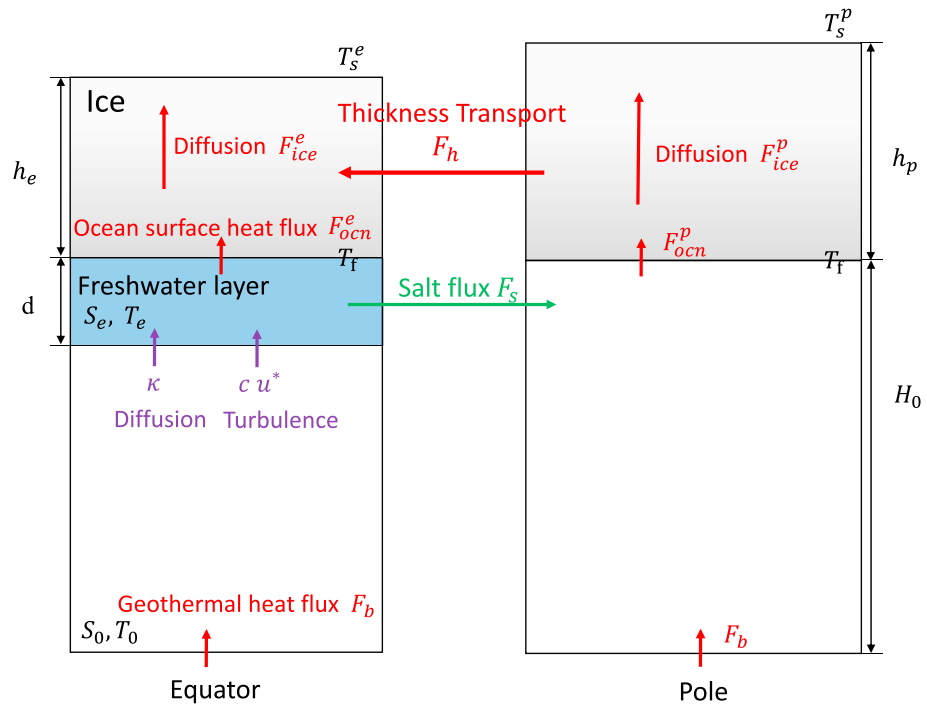


Figure 1. Model schematic depicting a (left) low-latitude and (right) high-latitude column. The uppermost (gray) boxes represent the ice shell. Heat is exchanged from the ocean to the ice, F_{ocn} (W m^{-2}), and is transported away from the ocean-ice interface by diffusion. The freshwater layer is denoted in blue, with salinity S^e , temperature T^e , and depth d . Red lines indicate heat transport, green lines indicate salt transport, and the purple lines indicate the transport of both temperature and salinity. F_b is the geothermal heat flux from the seafloor.

Relative variations in Europa's ice thickness ($\Delta h/h^e \sim 20\%$ [Nimmo *et al.*, 2007]) are much smaller than the variation of surface temperature ($\Delta T/T^e \sim 110\%$, Table 1). Thus, we can simplify the ice thickness equations by ignoring Δh in (2). The steady state thickness flux can then be estimated from (1) and (2) as

$$F_h = \frac{\kappa_{ice}(T_s^e - T_s^p)}{2h_0L} + \frac{\Delta F_{ocn}}{2L}. \quad (3)$$

Thus, the thickness flux is energetically constrained by the meridional gradients in both ice surface temperature and ocean-ice heat fluxes. The two factors positively contribute to the transport if the ocean-ice heat fluxes are greater at the equator as in Soderlund *et al.* [2014]. In contrast, a reduction (or disappearance) of the thickness flux occurs when the ocean-ice heat flux is greater at the poles, as argued by Jansen [2016].

This lateral ice transport is a key process that leads to freshwater accumulation at low latitudes. The resulting freshwater flux at the top of the ocean, F_s , is given by

$$F_s = S_0 \frac{\rho_i}{\rho} F_h, \quad (4)$$

where S_0 is the average salinity of Europa's ocean, and ρ_i and ρ are densities of ice and water, respectively (Table 1). Next, we examine the depth of the freshwater layer, which depends on the ocean's circulation.

2.2. Salt Balance in a Freshwater Layer

We simplify the meridional distribution of the freshwater layer by considering a layer with depth d in the low-latitude column and no freshwater layer in the high-latitude column. Thus, the ocean is partitioned into three regions or boxes (Figure 1), overlaid by the ice shell. The freshwater layer is represented by the upper equatorial box, with salinity S^e . We assume a uniform salinity S_0 for the rest of the ocean, which implies a circulation strong enough to keep the lower ocean well mixed and no additional sources of salt for the ocean.

To balance the melting at low latitudes due to the equatorward ice transport, ice forms (and rejects brine) at high latitudes. This is equivalent to a lateral salt flux out of the freshwater layer (F_s in Figure 1). Additionally,

Table 1. Freshwater Layer Model Parameters and Their Approximate Ranges

Symbol	Description	Value	Range	Unit
T_s^{ea}	Surface temperature at the equator	110	-	K
T_s^{pa}	Surface temperature at the pole	52	-	K
κ_{ice}	Thermal conductivity of ice	2	-	$W m^{-1} K^{-1}$
L	Latent heat of fusion of water	3.3×10^8	-	$J m^{-3}$
h_0	Equilibrium ice thickness at the equator	10	-	km
ρ	Density of pure water	1000	-	$kg m^{-3}$
ρ_i	Density of ice	920	-	$kg m^{-3}$
C_p	Specific heat capacity of water	4000	-	$J kg^{-1} K^{-1}$
β (NaCl) ^b	Haline contraction coefficient of aqueous NaCl	7.7×10^{-4}	$(6.4-7.8) \times 10^{-4}$	psu ⁻¹
β (MgSO ₄) ^c	Haline contraction coefficient of aqueous MgSO ₄	8.3×10^{-4}	$(6.6-10) \times 10^{-4}$	psu ⁻¹
α/β (NaCl) ^b	Ratio of α to β for NaCl	0.10	0–0.5	psu K ⁻¹
α/β (MgSO ₄) ^c	Ratio of α to β for MgSO ₄	0.18	0–0.42	psu K ⁻¹
g	Gravitational acceleration on Europa	1.3	-	$m s^{-2}$
κ	Effective diffusivity	10^{-4}	-	$m^2 s^{-1}$
F_b^d	Geothermal heat flux	0.01	0.01–0.1	$W m^{-2}$

^aTravis *et al.* [2012].

^bMcDougall and Barker [2011].

^cVance and Brown [2013].

^dLowell and DuBose [2005]; Vance and Brown [2013].

turbulent salt and heat transport may occur across the interface between the layer and the deep ocean in response to the vertical velocity shear of a mean flow circulation, as suggested by Soderlund *et al.* [2014]. In a steady state, F_s is balanced by turbulent mixing and diffusion of salt from the deep ocean. This balance can be written in the following way:

$$(cu^* + \frac{\kappa}{d})\Delta S = (S_0 - \Delta S)\frac{\rho_i}{\rho}F_h, \quad (5)$$

where c is the entrainment rate (or the efficiency of turbulent mixing) at the interface of the freshwater layer and the deep ocean, u^* is the characteristic velocity of turbulent fluctuations at the interface, and κ is an effective diffusivity representing tracer transport due to other processes (e.g., molecular diffusion or mixing by convecting plumes).

Vertical stratification suppresses the efficiency of turbulent transport, and the entrainment rate is commonly parameterized as a power law function of the bulk Richardson number, Ri . Following, e.g., Kit *et al.* [1980] and Manucharyan and Caulfield [2015], we assume the following dependencies:

$$c = 1.5Ri^{-3/2}, \quad Ri = \frac{dg\beta\Delta S}{u^{*2}}, \quad \Delta S = S_0 - S^e. \quad (6)$$

The Richardson number defines the ratio of the vertical stratification (reflected by a salinity contrast ΔS) to the vertical velocity shear and indicates (for $Ri \gg 1$) the stratification's ability to suppress turbulent mixing (equation (6)). Vertical heat transport at the ice-ocean interface at low latitudes is parameterized in the same way, i.e., $F_{ocn}^e = \rho C_p c_{ice} u^* (T_e - T_f)$, where c_{ice} is the entrainment rate at the ice-ocean interface at low latitudes and has a fixed value.

Since the freshwater layer is in direct contact with the ice, its near-freezing temperature and low salinity have opposing effects on buoyancy. The relative importance of salinity and temperature is expressed through the ratio $\alpha\Delta T/\beta\Delta S$, where β and α are the saline and thermal expansion coefficients, respectively (Table 1). When this ratio is small, we can approximate the buoyancy contrast as $\Delta b = g\beta\Delta S$, which yields the relationship for Ri in (6). Combining the definition of ΔS in (6) with (5), c , Ri , and ΔS can be determined as functions of average salinity S_0 , freshwater layer depth d , and the turbulent velocity u^* . Below, we explore the parameter regimes under which the freshwater layer can affect the stratification and heat content of Europa's ocean.

3. Results

3.1. Meridional Thickness Flux of Ice

We assume that in steady state, the polar ocean-ice heat flux is equivalent to the geothermal heat flux at the seafloor (i.e., $F_{\text{ocn}}^p = F_b$). A range of F_b has been applied in studies of Europa's ocean (section 4; Table 1). Here we adopt a reference value of $F_b = 0.01 \text{ W m}^{-2}$. The thickness flux F_h depends on equator-to-pole differences in the ice surface temperature and the heat flux at the ocean-ice interface (equation (3)). If we assume the equatorial heat flux to be 40% larger than at the poles (i.e., $\Delta F_{\text{ocn}}/F_{\text{ocn}}^p = 0.4$) as in Soderlund *et al.* [2014], then the two terms in equation (3) contribute comparably to F_h , $O(10^{-11}) \text{ m s}^{-1}$, or $\sim 7 \times 10^{-4} \text{ m yr}^{-1}$. Note that a strong ocean-ice heat flux at the poles ($\Delta F_{\text{ocn}} < 0$) can overcome the positive surface temperature term, and the thickness transport can become poleward ($F_h < 0$), leading to freshwater formation at high latitudes. The mathematical descriptions for the freshwater layer located either at the poles or the equator are equivalent after switching the locations of the boxes in the schematic (Figure 1). Here we consider a meridionally uniform distribution of the ocean-ice heat flux ($\Delta F_{\text{ocn}} = 0$), which leads to $F_h = 1.76 \times 10^{-11} \text{ m s}^{-1}$ and a freshwater layer at low latitudes. We discuss the sensitivity of the stratification to F_h and other model parameters in section 3.4.

3.2. Critical Ranges of the Freshwater Layer Depth

To determine the requisite conditions for a freshwater layer from the salinity balance, (5) and (6), additional constraints are needed. First, solutions for ΔS must be real and positive. This puts a lower bound on the layer thickness, d_{min} . Second, turbulent mixing should be weaker at the base of the freshwater layer than at the ocean-ice interface when stratification is strong enough to suppress mixing at the former location. Assuming a uniform turbulent velocity u^* across the layer implies $c < c_{\text{ice}}$. This is the condition that defines a distinct freshwater layer. A system with $c \gg c_{\text{ice}}$ would not affect the deep ocean heat content because the heat would be efficiently mixed into the upper ocean. Here we set $c_{\text{ice}} = 10^{-3}$ [McPhee *et al.*, 1999; Jenkins, 1991] (see supporting information for details). The requirement $c < c_{\text{ice}}$ puts an upper bound on the layer thickness, d_{max} . Finally, we require the layer to be buoyant, i.e., $\alpha \Delta T < \beta \Delta S$. In the analytical derivation below, we assume that salt transport into the layer is dominated by the stratified turbulence, i.e., $cu^* \gg \kappa/d$ in (5). Numerical solutions that include all the terms in (5) (Figure 2) show that this last condition is satisfied for $d_{\text{min}} < d < d_{\text{max}}$.

Combining (5) and (6), and using the assumption that $cu^* \gg \kappa/d$, we obtain

$$d_{\text{min}} = \frac{0.84u^{*8/3}}{\left(\frac{\rho_l}{\rho} F_h\right)^{2/3} g \beta S_0}. \quad (7)$$

Details of the derivation are available in the supporting information. Given the second criterion, $c < c_{\text{ice}}$, using the definitions for c (6) and $c_{\text{ice}} = 10^{-3}$, and assuming $S_0 \gg \Delta S$ results in

$$d_{\text{max}} = \frac{0.13u^{*3}}{\frac{\rho_l}{\rho} F_h g \beta S_0}. \quad (8)$$

Figure 2 shows solutions of the full salinity balance equations (5) and (6) at $S_0 = 50 \text{ psu}$, $F_b = 0.01 \text{ W m}^{-2}$ and $F_h = 1.76 \times 10^{-11} \text{ m s}^{-1}$ for seawater (aqueous sodium chloride); these conditions satisfy all three requirements above. For a given u^* , a range of freshwater layer depths is permitted. The colored region represents the parameter space where ΔS is real and positive. The white region is associated with parameters where the freshwater layer cannot be in a steady balance; instead, for a given u^* , turbulent mixing would cause the layer to deepen until it reaches d_{min} . This also explains the increase in d_{min} with stronger mixing. Both d_{min} and d_{max} strongly depend on the magnitude of turbulence, scaled approximately as u^{*3} according to (7) and (8). For the freshwater layer to be less than the total depth of the ocean ($d_{\text{min}} < 100 \text{ km}$), the turbulence needs to be sufficiently weak (Figure 2), e.g., u^* should range from 0.001 to 0.02 m s^{-1} for the case in Figure 2.

For aqueous magnesium sulfate (MgSO_4) and sodium chloride (NaCl), the two major saline components that have been considered for Europa's ocean [Zolotov and Kargel, 2009], there is no significant difference in ΔS because of their similar thermodynamic properties (Table 1). Freshwater characteristics for a MgSO_4 ocean are provided in the supporting information (Figure S1). Within the critical range of d , ΔS for the seawater case above varies from 10^{-4} to 0.2 psu (Figure 2).

3.3. Temperature Contrast and Minimum Average Salinity

Ocean heat content depends not only on the geothermal heat flux but also on the efficiency of the heat exchange with the ice. The freshwater layer functions as a blanket that partially insulates the deep ocean

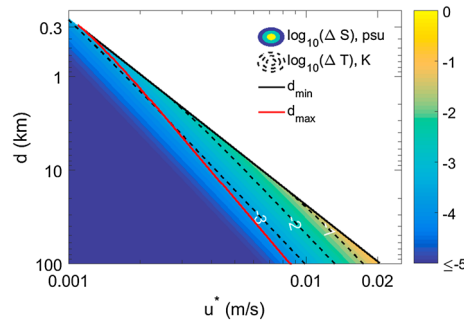


Figure 2. Salinity contrast ΔS (color-filled contours) and temperature contrast ΔT (dashed contours) between the deep ocean and the freshwater layer for seawater at an average salinity of 50 practical salinity units (psu). For these calculations $F_h = 1.76 \times 10^{-11} \text{ m s}^{-1}$ and $F_b = 0.01 \text{ W m}^{-2}$. The black and red contours indicate d_{\min} and d_{\max} , respectively. All ΔT and ΔS values are in \log_{10} space; u^* and d axes are logarithmic.

from the ice and may create a stronger vertical temperature gradient than an ocean without the layer. To quantify this insulating effect, we consider the heat budget of the deep ocean for which heat transport into the freshwater layer balances geothermal heating:

$$\frac{F_b}{\rho C_p} = \left(cu^* + \frac{\kappa}{d} \right) \Delta T. \quad (9)$$

Here $\Delta T = T_0 - T^e$ is the temperature difference between the deep ocean and the freshwater layer (Figure 1), which is nearly at the freezing temperature because it is in direct contact with the ice. This one-dimensional balance does not account for lateral heat transport between low- and high-latitude columns, which could be parameterized by introducing a lateral eddy diffusivity [e.g., Jansen, 2016], although the magnitude of this term is uncertain.

Combining (5), (6), and (9) and assuming $S_0 \gg \Delta S$, $cu^* \gg \frac{\kappa}{d}$ gives

$$\Delta T = \frac{F_b \Delta S}{C_p \rho_i F_h S_0} = \frac{2.25 \rho^2 F_b u^{*8}}{C_p (dg \beta \rho_i F_h S_0)^3}. \quad (10)$$

The real dependence of ΔT on u^* is obscured here because of the additional dependence of d on u^* . However, using (7) and (8), ΔT is independent of u^* for $d = d_{\min}$ and $\Delta T \sim u^{*-1}$ for $d = d_{\max}$. This is consistent with a weakening of ΔT in response to stronger mixing. Furthermore, ΔT increases linearly with ΔS , consistent with a stronger stratification insulating the deep ocean. For d within the critical range, ΔT ranges from $4 \times 10^{-4} \text{ K}$ to 0.6 K depending on the strength of turbulence (Figure 2). Thus, the insulating effect of the freshwater layer can increase the heat content of Europa's ocean.

However, the increase in deep ocean temperature (equation (10)) can destabilize the water column, counteracting the stabilizing effect due to salinity. Thus, satisfying the layer stability criterion $\alpha \Delta T < \beta \Delta S$ bounds the minimum salinity of the deep ocean:

$$S_0 > \frac{\alpha F_b}{\beta C_p \rho_i F_h}. \quad (11)$$

Accounting for the uncertainty of geothermal heat flux F_b (Table 1), the range of minimum S_0 is 28–200 psu and 16–100 psu for magnesium sulfate and seawater, respectively. This range of salinities is plausible; maximum salinities inferred from the induced magnetic field's amplitude are 200 psu for magnesium sulfate [Hand and Chyba, 2007] and 100 psu for seawater [Schilling et al., 2007]. Note that the minimum salinity requirement also varies with ΔF_{ocn} through its dependence on F_h (equation (3)).

3.4. Sensitivity to S_0 , F_b , and F_h

Here we examine the sensitivity of the freshwater-induced stratification to S_0 , F_b , and F_h , whose values vary within the ranges suggested by previous studies (Table 1). When the deep ocean is saltier, the freshwater layer tends to be thinner, i.e., d_{\min} and d_{\max} decrease with S_0 (equation (7) and (8)). This is because Ri is proportional to both d and ΔS ; a smaller d requires a larger ΔS to achieve the same mixing conditions (the same Ri value).

Figure 3a shows ΔT at the minimum depth of the layer as a function of F_b and S_0 , for seawater. Colored regions indicate where the buoyancy requirement (11) is satisfied. ΔT ranges from 0.1 to 0.7 K. The corresponding ΔS has smaller variations, 0.05 to 0.08 psu, and is not shown. The suppressing effect on heat transport between the layer and the deep ocean tends to be stronger (higher ΔT) when the deep ocean is less salty and has stronger geothermal heating. Moreover, F_b cannot be so high as to cause the minimum salinity of the deep ocean to exceed the maximum possible salinity. The upper limit of F_b is 0.072 W m^{-2} for MgSO_4 ocean and 0.065 W m^{-2} for seawater.

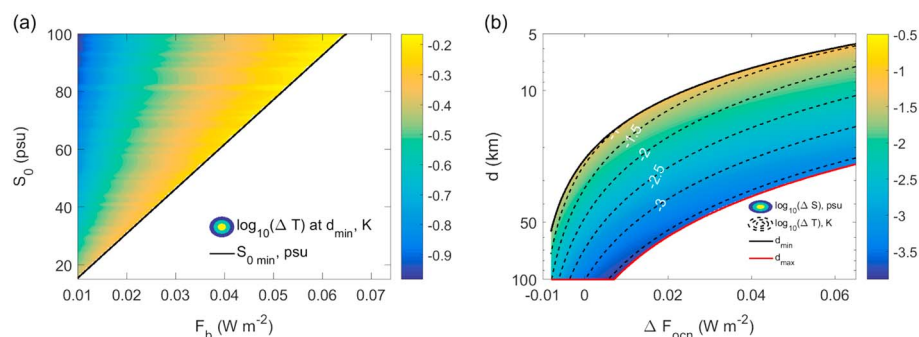


Figure 3. (a) Temperature contrast ΔT between the freshwater layer and the deep ocean corresponding to d_{min} , at $u^* = 0.01 \text{ m s}^{-1}$ and $F_h = 1.76 \times 10^{-11} \text{ m s}^{-1}$, for seawater, as a function of F_b and S_0 . The black contour indicates the minimum permissible salinity. ΔT is plotted in \log_{10} space. (b) Range of freshwater layer depth d , bounded by d_{min} and d_{max} (black and red contours, respectively), temperature contrast ΔT (dashed lines) and salinity contrast ΔS (colors) as a function of ΔF_{ocn} (W m^{-2}), for seawater at $S_0 = 50 \text{ psu}$, $u^* = 0.01 \text{ m s}^{-1}$, and $F_b = 0.01 \text{ W m}^{-2}$.

The ice thickness flux F_h is sensitive to ΔF_{ocn} (equation (3)) and therefore may also affect ΔT (Figure 3b). The results in this panel are calculated for seawater at $S_0 = 50 \text{ psu}$, $u^* = 0.01 \text{ m s}^{-1}$, and $F_b = 0.01 \text{ W m}^{-2}$. With these values, we find that ΔF_{ocn} may range from -0.008 to 0.065 W m^{-2} , where the lower bound arises from satisfying the condition that the minimum salinity is smaller than 50 psu. Consistent with (7) and (8), the upper and lower limits of d decrease with increasing F_h (i.e., increasing ΔF_{ocn}). This dependence reflects a stronger salinity contrast with increased supply of freshwater, which needs a thinner layer to achieve the same value of Ri . Within the critical depth range, ΔT varies from $2 \times 10^{-4} \text{ K}$ to 0.4 K and increases monotonically with F_h . The sensitivities of MgSO_4 ocean to S_0 , F_b , and F_h are very similar to seawater (Figure S2).

4. Discussion and Conclusions

The conceptual ice-ocean model developed here quantitatively explores the hypothesis that stratification in Europa's upper ocean can result from freshwater fluxes associated with meridional ice transport. We demonstrate that a meridional gradient in ice thickness can cause differential freezing of ice at the poles and melting at the equator, creating a freshwater flux at the top of the ocean. Over sufficiently long timescales, a persistent freshwater flux can form a diluted upper ocean layer or a "freshwater" layer under the ice shell at low latitudes. Density stratification at the base of the layer affects the turbulent exchange of heat and salt with the deep ocean. Under a wide range of parameters, the layer acts as a blanket that partially isolates the deep ocean from the ice shell, allowing it to efficiently accumulate heat from below. As a result, deep ocean temperatures can exceed the expected adiabat by $4 \times 10^{-4} \text{ K}$ to 0.6 K , depending on both the bulk characteristics of the layer and the turbulent properties of the ocean. As predicted by our model, the energetic circulation proposed by Soderlund *et al.* [2014] would prohibit the formation of a freshwater layer. However, other circulation regimes with weaker turbulence [e.g., Vance and Goodman, 2009; Jansen, 2016] could support a freshwater layer in Europa's ocean.

We describe both analytical and numerical solutions for the depth of the freshwater layer and for the magnitude of the vertical temperature and salinity contrasts. The critical depth range for freshwater layer formation is mainly controlled by the strength of upper ocean turbulence and is sensitive to the average salinity of Europa's ocean. With stronger turbulence and lower average salinity, the freshwater layer tends to extend deeper. A process that is not addressed in this model is the spreading of the freshwater layer to higher latitudes to counteract the lateral density gradient. The omission of this effect implies that freshwater layer depths calculated in this study are upper bounds.

The aim of the present conceptual model is to highlight key processes that can affect the heat and salt balances of the ocean. The model uses basic parameterizations of various physical processes, so it is important to note where its assumptions may lead to unphysical results. First, our model adopts a shear-driven parameterization of stratified turbulence. Because there are no observations of any properties of upper ocean turbulence in Europa, we devote further attention to different representations of the turbulent exchange at the layer interfaces in the supporting information [Baines, 1975; Shrinivas and Hunt, 2014; Kumagai, 1984] to demonstrate the similarity of our turbulent parameterization to that of vertical plume-driven turbulence. Our conclusions

are not sensitive to the choice of turbulent parameterization as long as the adopted parameterization causes stratification to suppress the efficiency of turbulent transport. Second, we neglect meridional heat transport via global overturning circulation or by ocean eddies, which can modify the differential ocean heat flux at the base of the ice shell (ΔF_{ocn}). These effects must be included to construct a fully coupled system for Europa's ice and ocean. This feedback cannot be determined at present due to the uncertainty in the nature of the circulation and heat transport processes in Europa's ocean. Nevertheless, the effects of lateral heat transport or other factors that influence F_h through ΔF_{ocn} (e.g., ice convection, tidal heating, and freezing point variations at the ice-ocean interface) can be determined from the sensitivity of the vertical stratification to ΔF_{ocn} (section 3.4). With the above caveats in mind, our model exhibits a broad parameter space under which a freshwater layer can exist. While some of those parameters are mutually dependent, our results are cause for further investigation of Europa's upper ocean stratification due to the global exchange of heat between Europa's ocean and ice.

Observations from NASA's planned Europa Clipper Mission [Pappalardo *et al.*, 2016] and ESA's planned Jupiter ICy satellite Explorer mission [Grasset *et al.*, 2013], will contribute to determining whether a freshwater layer exists, in particular by constraining the surface temperature distribution, the salinity of Europa's ocean, and variations in its ice thickness. Such findings may in turn offer insight into Europa's habitability by helping to constrain the fluxes of energy and potential nutrients between the ice and ocean.

Acknowledgments

P.Z. completed this work through Caltech's Summer Undergraduate Research Fellowship (SURF) program; we thank the organizers for their support. G.E.M. was supported by the Stanback Postdoctoral Fellowship Fund at Caltech. This work was partially supported by Strategic Research and Technology funds from the Jet Propulsion Laboratory, Caltech, and by the Icy Worlds node of NASA's Astrobiology Institute (13-13NAI7_2-0024). The research was carried out at the Jet Propulsion Laboratory, California Institute of Technology, under a contract with the National Aeronautics and Space Administration. The numerical model based on equations described in this paper produced figures that include all of the numerical information, so there are no data-sharing issues.

References

- Anderson, J., G. Schubert, R. Jacobson, E. Lau, W. Moore, and W. Sjogren (1998), Europa's differentiated internal structure: Inferences from four Galileo encounters, *Science*, 281(5385), 2019–2022.
- Baines, W. (1975), Entrainment by a plume or jet at a density interface, *J. Fluid Mech.*, 68(1), 309–320.
- Goodman, J. C., and R. T. Pierrehumbert (2003), Glacial flow of floating marine ice in “snowball earth”, *J. Geophys. Res. Oceans*, 108(C10), 3308.
- Goodman, J. C., G. C. Collins, J. Marshall, and R. T. Pierrehumbert (2004), Hydrothermal plume dynamics on Europa: Implications for chaos formation, *J. Geophys. Res.*, 109(E3), E03008, doi:10.1029/2003JE002073.
- Grasset, O., *et al.* (2013), JUJupiter ICy moons Explorer (JUICE): An ESA mission to orbit Ganymede and to characterise the Jupiter system, *Planet. Space Sci.*, 78, 1–21, doi:10.1016/j.pss.2012.12.002.
- Hand, K., and C. Chyba (2007), Empirical constraints on the salinity of the European ocean and implications for a thin ice shell, *Icarus*, 189(2), 424–438.
- Irwin, L. N., and D. Schulze-Makuch (2003), Strategy for modeling putative multilevel ecosystems on Europa, *Astrobiology*, 3(4), 813–821.
- Jansen, M. F. (2016), The turbulent circulation of a snowball Earth ocean, *J. Phys. Oceanogr.*, 46(6), 1917–1933.
- Jenkins, A. (1991), A one-dimensional model of ice shelf-ocean interaction, *J. Geophys. Res.*, 96(C11), 20,671–20,677.
- Kit, E., E. Berent, and M. Vajda (1980), Vertical mixing induced by wind and a rotating screen in a stratified fluid in a channel, *J. Hydraul. Res.*, 18(1), 35–58.
- Kivelson, M., K. Khurana, C. Russell, M. Volwerk, R. Walker, and C. Zimmer (2000), Galileo magnetometer measurements: A stronger case for a subsurface ocean at Europa, *Science*, 289, 1340–1343.
- Kumagai, M. (1984), Turbulent buoyant convection from a source in a confined two-layered region, *J. Fluid Mech.*, 147(1), 105–131.
- Lewis, E. L., and R. G. Perkin (1986), Ice pumps and their rates, *J. Geophys. Res.*, 91, 11,756–11,762.
- Lowell, R. P., and M. DuBose (2005), Hydrothermal systems on Europa, *Geophys. Res. Lett.*, 32(5), L05202, doi:10.1029/2005GL022375.
- Manucharyan, G. E., and C. Caulfield (2015), Entrainment and mixed layer dynamics of a surface-stress-driven stratified fluid, *J. Fluid Mech.*, 765, 653–667.
- McDougall, T. J., and P. M. Barker (2011), Getting started with TEOS-10 and the Gibbs Seawater (GSW) oceanographic toolbox, *SCOR/IAPSO WG*, 127, 1–28.
- McKinnon, W. B., and M. E. Zolensky (2003), Sulfate content of Europa's ocean and shell: Evolutionary considerations and some geological and astrobiological implications, *Astrobiology*, 3(4), 879–897.
- McPhee, M. G., C. Kottmeier, and J. H. Morison (1999), Ocean heat flux in the central Weddell Sea during winter, *J. Phys. Oceanogr.*, 29(6), 1166–1179.
- Melosh, H. J., A. G. Ekholm, A. P. Showman, and R. D. Lorenz (2004), The temperature of Europa's subsurface water ocean, *Icarus*, 168(2), 498–502.
- Nimmo, F., and R. Pappalardo (2016), Ocean worlds in the outer solar system, *J. Geophys. Res. Planets*, 121(8), 1378–1399.
- Nimmo, F., P. Thomas, R. Pappalardo, and W. Moore (2007), The global shape of Europa: Constraints on lateral shell thickness variations, *Icarus*, 191(1), 183–192.
- Pappalardo, R., L. Prockter, D. Senske, R. Klima, S. Fenton Vance, and K. Craft (2016), Science objectives and capabilities of the NASA Europa Mission, in *Proceedings of the 47th Lunar and Planetary Science Conference*, pp. 3058, The Woodlands, Tex.
- Pappalardo, R. T., *et al.* (1998), Geological evidence for solid-state convection in Europa's ice shell, *Nature*, 391(6665), 365–368.
- Rathbun, J., N. Rodriguez, and J. Spencer (2010), Galileo PPR observations of Europa: Hotspot detection limits and surface thermal properties, *Icarus*, 210(2), 763–769.
- Schilling, N., F. M. Neubauer, and J. Saur (2007), Time-varying interaction of Europa with the Jovian magnetosphere: Constraints on the conductivity of Europa's subsurface ocean, *Icarus*, 192(1), 41–55.
- Schulze-Makuch, D., and L. N. Irwin (2002), Energy cycling and hypothetical organisms in Europa's ocean, *Astrobiology*, 2(1), 105–121.
- Shrinivas, A., and G. Hunt (2014), Unconfined turbulent entrainment across density interfaces, *J. Fluid Mech.*, 757(1), 573–598.
- Siegert, M., J. Ellis-Evans, M. Tranter, C. Mayer, J. Petit, A. Salamatin, and J. Priscu (2001), Physical, chemical and biological processes in Lake Vostok and other Antarctic subglacial lakes, *Nature*, 414, 603–609.
- Soderlund, K., B. Schmidt, J. Wicht, and D. Blankenship (2014), Ocean-driven heating of Europa's icy shell at low latitudes, *Nat. Geosci.*, 7(1), 16–19.

- Spencer, J. R., L. K. Tamppari, T. Z. Martin, and L. D. Travis (1999), Temperatures on Europa from Galileo photopolarimeter-radiometer: Nighttime thermal anomalies, *Science*, *284*(5419), 1514–1516.
- Thomson, R. E., and J. R. Delaney (2001), Evidence for a weakly stratified European ocean sustained by seafloor heat flux, *J. Geophys. Res.*, *106*(E6), 12,355–12,365.
- Travis, B., J. Palguta, and G. Schubert (2012), A whole-moon thermal history model of Europa: Impact of hydrothermal circulation and salt transport, *Icarus*, *218*, 1006–1019.
- Vance, S., and J. Brown (2013), Thermodynamic properties of aqueous MgSO_4 to 800 MPa at temperatures from -20 to 100°C and concentrations to 2.5 mol kg^{-1} from sound speeds, with applications to icy world oceans, *Geochim. Cosmochim. Acta*, *110*, 176–189.
- Vance, S., and J. Goodman (2009), Oceanography of an ice-covered moon, in *Europa*, pp. 459–482, Arizona Univ. Press, Tucson, Ariz.
- Vance, S., K. Hand, and R. Pappalardo (2016), Geophysical controls of chemical disequilibria in Europa, *Geophys. Res. Lett.*, *43*(10), 4871–4879, doi:10.1002/2016GL068547.
- Zahnle, K., J. L. Alvarillos, A. Dobrovolskis, and P. Hamill (2008), Secondary and sesquinary craters on Europa, *Icarus*, *194*, 670–674.
- Zolotov, M., and E. Shock (2001), Composition and stability of salts on the surface of Europa and their oceanic origin, *J. Geophys. Res.*, *106*(E12), 32,815–32,828.
- Zolotov, M. Y., and J. Kargel (2009), On the chemical composition of Europa's icy shell, ocean, and underlying rocks, in *Europa*, edited by R. T. Pappalardo, W. B. McKinnon, and K. Khurana, pp. 431–458, Univ. Arizona Press, Tucson, Ariz.